International Journal of Thermal Sciences 49 (2010) 409–417

Contents lists available at ScienceDirect

International Journal of Thermal Sciences

journal homepage: www.elsevier.com/locate/ijts

Application of spray impingement technique for characterisation of high pressure sprays from multi-hole diesel nozzles

D.K. Sangiah*, L.C. Ganippa

School of Engineering and Design, Brunel University, Uxbridge, UK

ARTICLE INFO

Article history:
Received 19 September 2008
Received in revised form
15 July 2009
Accepted 10 August 2009
Available online 26 August 2009

Keywords:
Impingement
Multi-hole
Nozzles
Transients

ABSTRACT

An attempt has been made to study and characterise the performance of two multi-hole nozzles of different nozzle hole geometry using the impingement technique. The technique was able to characterise the nozzle geometry and the near nozzle spray characteristics. The transients of the needle motion, dynamics of the pressure fluctuations were all reflected in the momentum flux measurements. The impingement distance had no significant effect on the derived injected fuel mass and the nozzle discharge coefficient. The momentum of the spray was observed to be strongly dependant on the fluctuations of the injection pressure but the average nozzle discharge coefficient for an orifice was not significantly influenced by different injection pressures. Numerous transients were observed to occur in the spray parameters over a single injection cycle and the transients in the spray were unique for an orifice and varied from one orifice to another in the same nozzle. This technique proves to be a vital tool for predicting the transient performance of high pressure nozzle flows.

1. Introduction

Emissions from engines have caused concerns due to global warming, degradation of environment and adverse health effects. In response to climate change phenomena, governing bodies in United States and Europe have proposed stringent emissions regulations on the automotive industries to meet targets in the foreseeable future. The key parameters that contribute to air pollution from engines are nitrogen oxides (NO_x), carbon monoxide (CO), hydro carbons (HC) and particulate matter (soot). These emissions are the consequence of inefficient combustion and have an undesirable effect on public health and the environment. Automotive industries are seeking different solutions to meet the stringent emission regulations. One of the preferred methods is to find a solution by controlling the combustion process and making it as efficient as possible. Solutions via after treatments tend to be overlooked by some engine manufactures, as they lead to increased components and hence high cost of production, maintenance and regeneration. The production of CO_2 is inevitable in engines as it is a product of combustion, but the stringent steps taken to meet the regulations contributes to the reduction in CO_2 emissions. However after treatment, additives and alternative fuel prove to be a better solution to reduce CO_2 emissions. In addition to complying to the emission regulations, the other important criteria that the industry tries to achieve is to improve the fuel consumption. Any reduction in fuel consumption has a significant effect on the maintenance cost of the vehicles and the fuel economy.

The ability to control the quantity of fuel injected into the combustion chamber in diesel engines opens the door for extensive research in optimising the combustion process. Research has lead to technical developments which have resulted in state of the art injection systems and engine control systems which combine to produce efficient combustion system with low emissions and fuel consumption. The common rail diesel fuel injection system is a typical example which has lead to controlled combustion and significant reduction in emissions and fuel consumption. The system is capable of generating very high pressures and also having a significant control over the injection quantity and injection timing. The common rail injectors possess significantly smaller orifice area and hence increased number of orifices in the nozzle. The characteristics of the injector together with ability of producing very high pressures, in the range of 2000 bar, increases air entrainment and enables better mixing of fuel with air.

Characterizing the behaviour of the spray inside the combustion chamber and the significance of orifice geometries has become a prime importance in recent years as it determines the fuel-air mixing and the spray combustion process. Various techniques are being used to study the spray mixing phenomena. The most extensively used application is the optical method where the spray is injected into a nitrogen filled combustion chamber, which is illuminated using laser

* Corresponding author.
E-mail address: sdhinesh2002@yahoo.co.uk (D.K. Sangiah).

1290-0729/$ – see front matter © 2009 Elsevier Masson SAS. All rights reserved.
doi:10.1016/j.ijthermalsci.2009.08.001

as a light source. The scattering signal from the fuel droplets in the spray is imaged using the state of the art high speed digital cameras, which can be analysed further. In order to correlate the spray patterns with the emissions, the injectors are tested under the same conditions in a conventional diesel engine. Flow rigs are another type of application which characterises the spray and orifice geometries by measuring the mass flow rate of the injectors.

The impingement technique is the most simplified application used to characterise spray and nozzle geometries. This technique is based on measuring the instantaneous force (momentum flux) of the injected fuel jet on a normally mounted sensor. The momentum of the spray strongly influences several important factors such as spray penetration, spray cone angle and air entrainment [1]. Spray momentum provides information about the mass flow rate and the flow exit velocity and it also controls the fuel-air mixing process [2]. The discharge coefficient can also be evaluated from the momentum flux measurements and is considered to be the most important functional parameter that governs the nozzle flow of an injector over the entire operating range [3]. The discharge coefficient (C_d) is defined as the ratio between the actual flow passing through the orifice to the flow that would pass through the same orifice at that pressure drop if the flow is frictionless and without any contraction or phase changes. The discharge coefficient depends on the properties of the flow and that of the fluid and of the nozzle geometry [3].

The impingement technique has been successfully used in the past by other authors [2–5] to determine the spray momentum flux, orifice discharge coefficients, injection rates, jet velocities, spray penetrations and the transients that exist during an injection cycle. However, limited work has been done to determine the momentum characteristics of multi-orifice nozzles with different geometrical configurations. Thus, this work will extend the database of the existing literature to characterise the nozzle geometry effects on the sprays that are injected from two multi-orifice nozzles for different fuel injection parameters.

2. Theory and calibration

The main objective of this study is to determine the discharge coefficient, injection rate and the instantaneous velocity of the spray from the momentum flux and injection pressure measurements for two different nozzles of different nozzle hole geometries. The fundamental equations relating these characteristic parameters were obtained from the Newton's Second Law and the Continuity Equations.

According to Newton's Second Law:

$$F(t) = \dot{m}(t)\cdot\Delta V(t) \tag{1}$$

Where $F(t)$ is the instantaneous impingement force, $\dot{m}(t)$ is the mass flow rate, and $\Delta V(t)$ is the change in velocity. In reality the collision of fuel droplets on the impingement transducer is an extremely complex process. In order to make the analysis simpler, the rebound velocity of the spray droplets after impact are assumed to be negligible compared to their injected velocity. So in this analysis the change in velocity is approximated to the velocity $V(t)$ of the spray before impact at that point along the spray axis. Since the momentum of the spray is destroyed at the sensor surface, the forces measured by the sensor can be considered to be equivalent to spray momentum flux. By applying Continuity and Bernoulli's equations at the exit of the orifice of the nozzle, the discharge coefficient can be derived as:

$$C_d = \frac{\dot{m}(t)}{\dot{m}_{\text{theo}}(t)} = \left[\frac{F(t)}{2\cdot A_0\cdot\Delta P(t)}\right]^{\frac{1}{2}} \tag{2}$$

where A_0 is the cross sectional area of the flow and $\Delta P(t)$ is the change in pressure (Injection pressure–back pressure). Detailed derivations of equation (2) are provided in [3–5].

Instantaneous discharge coefficient will provide information regarding the dynamic changes that are occurring in the nozzle flow during the short injection time period of few milliseconds. In addition to capturing the dynamic changes in the nozzle flow, information regarding the nozzle internal geometry can also be inferred through the nozzle discharge coefficient. Thus, the impingement technique will provide information regarding the nozzle discharge coefficient, injection rate and the instantaneous velocity of the spray at any time (t) and the cumulative mass flow from an orifice, per injection cycle.

A piezo-electric pressure transducer, Kistler (Type-601A), was used for the impingement measurements and the output from the transducer was amplified by a Kistler charge amplifier (Type 5009). The transducer was mounted on a test bench with its diaphragm protruding, in a horizontal vise and it was force calibrated. Calibrated weights of 0.5 N, 1 N and 2 N were used for the calibration process. These weights were chosen as they are in the same range as the forces exerted by a single injector spray [1,2,5]. A total of 50 readings were obtained for each calibrated weight and their mean values were used for calibrating the transducer for the momentum flux measurements. The principle of the spray impingement technique is shown schematically in Fig. 1.

3. Experiments

The schematic of the developed spray impingement test rig together with the high pressure common rail fuel injection system is shown in Fig. 2. The fuel system compromised of a fuel tank, fuel lift pumps and a motor driven high pressure common rail pump. The injection system is capable of generating pressures up to 1500 bar. The lift pump was used to supply fuel to the high pressure pump as the fuel tank was at the lowest point in the hydraulic system. An instrumentation rack consisting of a computer and an injector driver unit was used to drive the injector in the impingement rig. The Em-tronichs programme was used to control the pump and the injector driver unit. A separate computer with an integrated data acquisition system was used for data acquisition. The data acquisition system consists of a high speed data acquisition card, SCB-68 and Lab View programme was used as the driver software. Lab View was programmed to acquire the input signals and collate the acquired data. The injection signal, impingement signal and the pressure transducer signals were measured using the

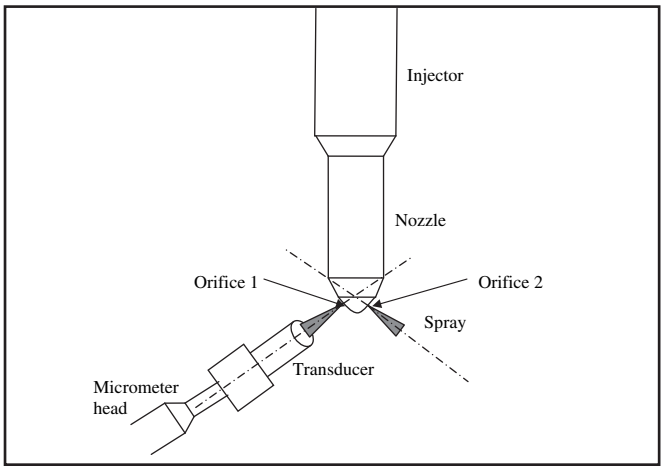

Fig. 1. Schematic of the spray impingement technique.

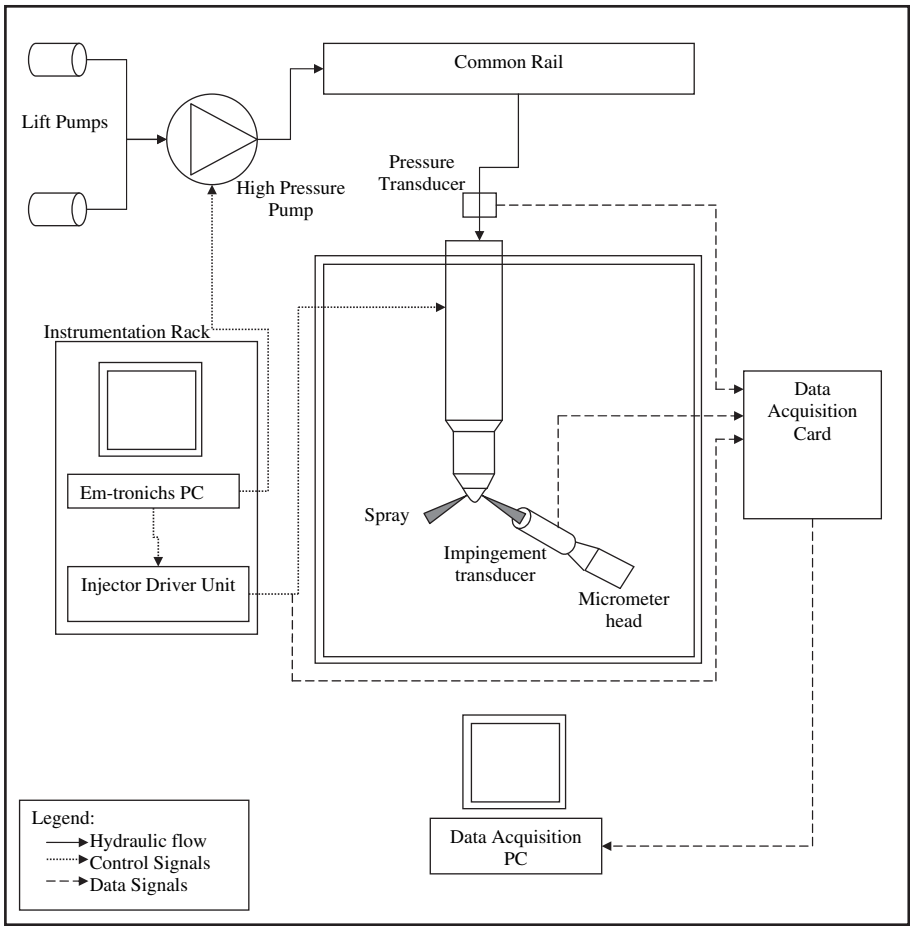

Fig. 2. Schematic of the experimental set-up.

data acquisition system. The pressures that is measured upstream of the injector has been approximated to the injection pressure at the tip of the nozzle orifice as it is assumed that when the needle opens, the pressure losses due to flow restrictions between the pressure transducer mounted on the fuel pipeline and the nozzle tip are negligible as also discussed by Siebers and Higgins [6]. The spray impingement distance (the axial distance between the nozzle tip and the sensor surface) was varied to study the influence of spray impingement distance on the momentum flux and other characteristic parameters. A micrometer screw gauge was used to measure the axial position of the transducer. The Transducer was directly assembled on to the head of the micrometer. Care was taken to align the transducer to the spray axis to make sure that all of the spray was impinging on the diaphragm of the transducer at all operating points.

The impingement measurements were carried out at the injection pressures of 600, 800 and 1000 bar for two different two hole nozzles (nozzle-0 and nozzle-1) using low sulphur diesel fuel having a density of about 845 kg m^{-3}. The sensor was placed at a distance of 0.5 mm, 1 mm and 2 mm from the nozzle tip and the whole set-up was enclosed in an atmospheric chamber. The atmospheric conditions used for the experiments are adequate to predict nozzle characteristics and the evaporation effects are not considered in this investigation. Moreover the position sensor is close to the nozzle tip and at this point the variations in vaporization are negligible. This can be depicted from Siebers et al. [6]".

The impingement distances were also chosen to ensure that the whole of the spray was captured on the diaphragm of the impingement transducer. The hole diameters for the two nozzles (nozzle-0 and nozzle-1) is 0.132 mm and 0.145 mm respectively. These nozzles have a different diameter but the same K-factor of 2.25 and an inlet hydro-grinding (honing) of 15%. The K-factor is a measure for the conicity of the orifice, where positive K-factors mean that the orifice narrows towards the exit of the nozzle. The intensity of cavitation in rounded inlet holes of the nozzles are relatively less compared to sharp inlet nozzles. However at different flow conditions the possibility of variations in cavitation intensity is very likely.

4. Results and discussions

The impingement measurements were carried out for each test conditions and were repeated 3 times to ensure the repeatability of the measurements but in this section the results were not averaged and the results for one complete injection are discussed. This section focuses on variations of the spray momentum flux, nozzle discharge coefficient, injection rate, injection velocity and discusses about the influence of injection pressure and the impingement distance on the above parameters. The orifice to orifice variations and the nozzle geometry effects on the characteristic parameters that are obtained from the spray impingement measurements are also discussed.

In this work the surrounding pressures are maintained at atmospheric conditions. It has been shown by Choeng et al. [7] that at high injection pressures a slight change in ambient conditions showed only minimal effect on the penetration of the spray since

the injection pressures are very high compared to back pressures. Thus, for the impingement technique, the effect of back pressure will be minimal on all the results discussed in this section.

4.1. Momentum flux

4.1.1. Time resolved momentum flux

The transient variations of momentum flux over the entire injection period for each orifice of the two nozzles (nozzle-0 and nozzle-1) are shown in Figs. 3 and 4. The momentum flux was observed to increases shortly after the opening of the injector needle, the instant at which the flow emerges out through the orifices. After a time period of about 0.7 ms the momentum flux peaks, which roughly corresponds to the instant at which the needle reaches its maximum lift position, and beyond this point the momentum flux was observed to drop due to the fluctuations of the rail pressure. These effects could be attributed to the dynamics of needle opening within a short time period of about few milliseconds (ms) and the associated propagation of pressure waves within the system. Towards the end of injection the momentum flux increases, which could be attributed to the start of closing of the needle and then decreases in time and reaches zeros, as the needle completely closes the nozzle orifice flow. In Figs. 3 (b) and 4 (a), (b) it could be seen that as the needle opens (the momentum flux increases) the rail pressure drops by about 15% and reaches its minimum shortly after the first peak of the momentum flux. As the injection pressure recovers the momentum flux decreases and eventually increases and reaches its peak, when the injection pressure recovers to its maximum after the first drop (of about 1 ms) after the start of injection. The momentum flux is at its maximum during the middle of the injection time period, and thereafter the momentum gradually drops for the rest of the injection cycle until the needle starts to closes. It was also observed that the fluctuation of injection pressure has a direct impact on the momentum flux during the intermediate stages of the injection. The momentum flux was not smooth and it was observed to be fluctuating during the intermediate stages of the injection period. This variation could be the combined effects of the fluctuations of the pressure in the system and the development of in stationary flow caused by the vibrations and dynamics of the needle lift.

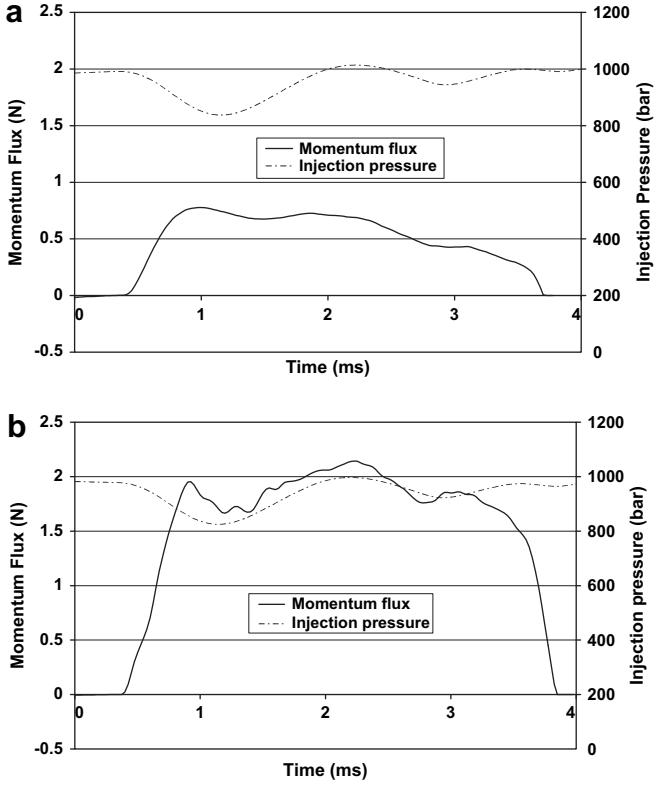

Fig. 3. (a) The momentum flux of spray from orifice1 of nozzle-0 at an injection pressure of 1000 bar measured at a distance of 0.5 mm from the nozzle tip. (b) The momentum flux of spray from orifice2 of nozzle-0 at an injection pressure of 1000 bar measured at a distance of 0.5 mm from the nozzle tip.

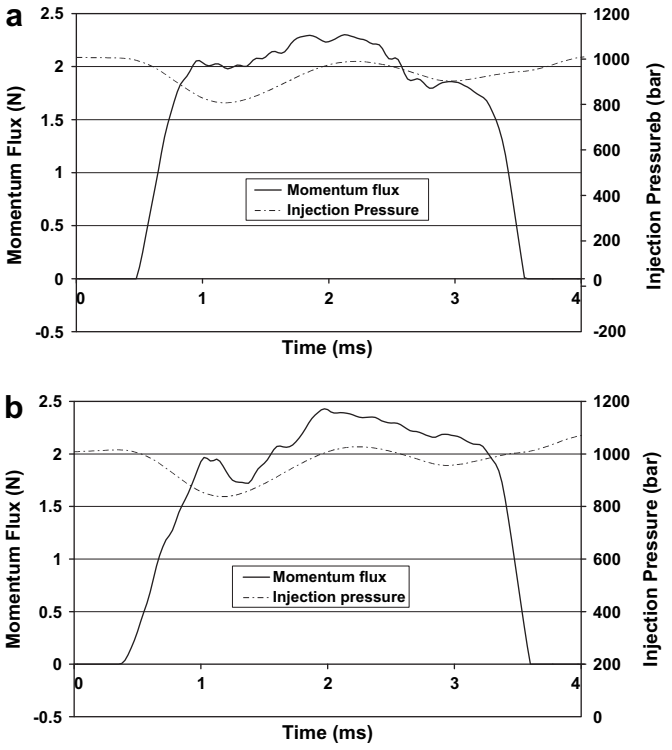

Fig. 4. (a) The momentum flux of spray from orifice1 of nozzle-1 at an injection pressure of 1000 bar measured at a distance of 0.5 mm from the nozzle tip. (b) The momentum flux of spray from orifice1 of nozzle-2 at an injection pressure of 1000 bar measured at a distance of 0.5 mm from the nozzle tip.

The magnitude of the momentum flux of orifice1 of nozzle-0, Fig. 3 (a), was observed to be significantly lower than other orifices and the corresponding profile of the momentum flux over the complete injection period was very different compared to all other orifices as shown in Figs. 3 (b) and 4 (a), (b). The momentum flux was also observed to reach its peak at the initial stage of the injection (as the needle opens) and then gradually drops until the injection ends. It appears that the flow in this orifice has been impeded either due to a blockage or due to some fault in the production of that hole of the orifice. The blockage or the defect in the orifice has a profound effect on the nozzle flow and the spray characteristics of that orifice as well as the other orifice of the same nozzle, as it is likely to increase the flow in order to conserve the mass flow rate. The profiles of the momentum flux of the sprays from the orifice2 of nozzle-0, Fig. 3 (b) and the two orifices of nozzle-1, Fig. 4 (a), (b) were observed to be globally similar. In Fig. 4 (a) it could be observed that the magnitude of the initial peak of the momentum flux of the spray emerging from orifice1 of nozzle-1 (after a time of 0.7 ms from the start of injection) was observed to be maximum relative to the other orifices. Also the drop in the momentum flux after the initial peak (after the time of 1 ms) was observed to be minimal for this orifice. In Fig. 3 (a) it could be seen

that the drop in the momentum flux of the jet after its initial peak (at 0.55 ms) was observed to be minimal compared to other orifices.

Numerous transients were observed during this short injection period. All the dynamic effects of injection pressure fluctuations, all the effects of needle motion and all the flow effects in the nozzle sac and the nozzle hole were all captured in the momentum flux measurement. The fluctuations that were seen in the injection pressure had a significant influence on the momentum flux measurements. The profiles of the characteristic parameters obtained from the impingement measurements and the magnitude of the results are similar to previous studies, Husberg et al. [4] and Desantes et al. [5].

4.1.2. Injection pressure effects on average momentum flux

In order to study the influence of injection pressure effects on the momentum flux, the time averaged momentum flux data was considered for different injection pressures. The average value at each operating point was obtained by determining the mean of the instantaneous values that were obtained during the intermediate stages of the complete injection process. Fig. 5 shows the variations of the time averaged momentum flux at different injection pressures at an impingement distance of 0.5 mm. The momentum flux for all the orifices was observed to increase linearly with the injection pressure. It could be seen that at higher injection pressures there was a considerable increase in the momentum flux. As observed earlier in the previous section, the momentum flux for orifice1 of nozzle-0 was significantly lower compared to all other orifices under all injection pressures. The momentum flux of the jet for the orifices of nozzle-1 was observed to be considerably higher than that of the orifices of nozzle-0 under all operating points. It can be clearly seen that for nozzle-0 there is a considerable difference in the momentum flux between the two orifices, but for nozzle-1 the differences are negligible. The differences in momentum flux between the nozzles are more pronounced than the differences observed between the orifices of nozzle-1.

4.2. Discharge coefficient

4.2.1. Time resolved nozzle discharge coefficient

From the momentum flux and the injection pressure data the nozzle discharge coefficient for each orifices were calculated using equation (2). The transient variations of C_d over the entire injection period for all the orifices are shown in Figs. 6 and 7, respectively. The defect that was observed in the orifice1 of nozzle-0 has been reflected in the measured orifice discharge coefficient. The orifice1 of nozzle-0 has the lowest C_d over the entire injection period and the

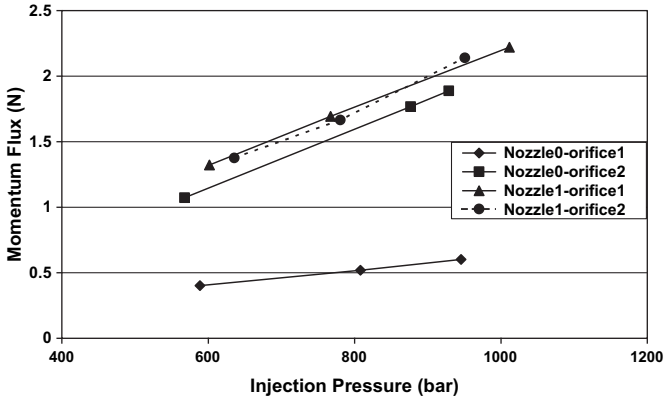

Fig. 5. Variation of average spray momentum flux measured at an impingement distance of 0.5 mm from nozzle tip at different injection pressures.

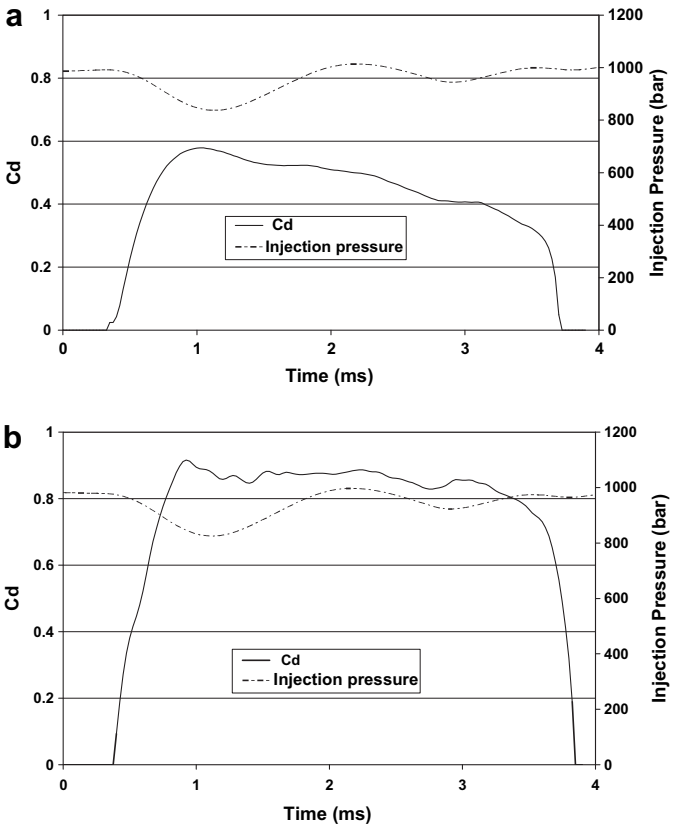

Fig. 6. (a) Variation of nozzle discharge coefficient for orifice1 of nozzle-0 at an injection pressure 1000 bar. (b) Variation of nozzle discharge coefficient for orifice2 of nozzle-0 at an injection pressure 1000 bar.

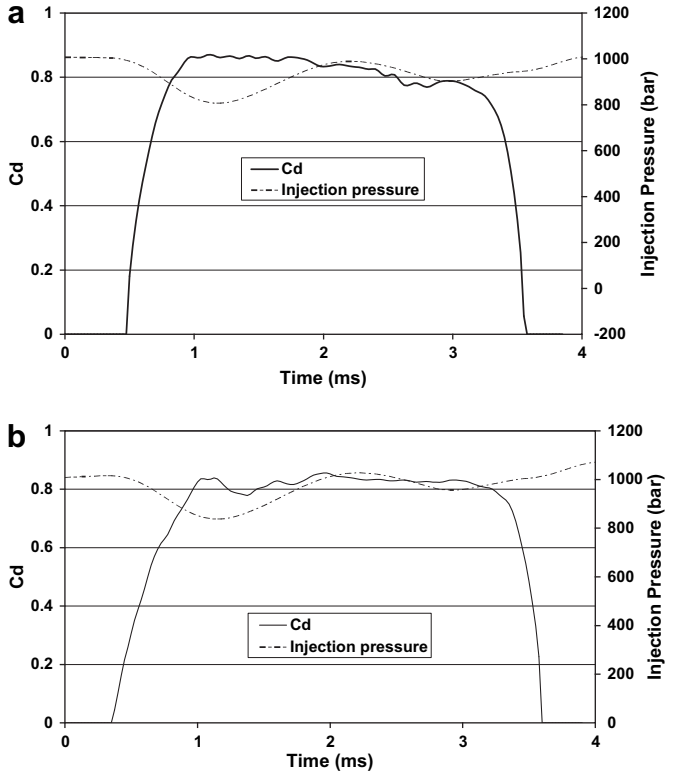

Fig. 7. (a) Variation of nozzle discharge coefficient for orifice1 of nozzle-1 at an injection pressure 1000 bar. (b) Variation of nozzle discharge coefficient for orifice2 of nozzle-1 at an injection pressure 1000 bar.

profile of the C_d curve is very different compared to all other orifices. After reaching its maximum of 0.57, it was observed to gradually decrease over the complete injection period until the nozzle closes. For all other orifices, in general, C_d was observed to be greater (in the range of 0.8–0.87) during the initial stages of the injection as the needle opens. The discharge coefficient gradually decreases during the intermediate stages of injection and was also observed to marginally increase and then decrease to zero when the needle started to close the orifice opening. Similar variations of higher C_d during the start and end of the injection cycle for the normally functioning orifices had been reported by Ganippa et al. [3].

Unlike the momentum flux, the injection pressure fluctuations have no significant effect on the C_d. For the orifice2 of nozzle-0 the C_d immediately drops after its initial peak (at 0.55 ms) and remains constant through the intermediate stages of injection before it slightly dips and increases again at the closing stages. The orifice1 of nozzle-1 was observed to remain at its peak value for a considerable amount of time during the initial stages of injection and then gradually drops to a considerable amount before slightly increasing at the closing stages of the injection. For orifice2 of nozzle-1, C_d was observed to drop and recover back and remain nearly constant during the rest of the injection period until the closing of the needle. Apart from orifice1 of nozzle-0 all the other three orifices have no pronounced difference in the trends for the variations of the nozzle discharge coefficient during the injection period.

The magnitude of C_d was observed to be highest (in the range of 0.87) for orifice2 of nozzle-0 for the entire injection period compared to all other orifices. Moreover the discharge coefficient for all the three orifices were generally in the range from 0.8 to 0.87, similar magnitudes ranges of C_d were reported by Ganippa et al. [3] and Husberg et al. [4].

A low value of C_d (maximum of 0.57) was observed by the orifice1 of nozzle-0, which could be due to the effect of blockage or production fault, which eventually impeded the flow and as result of which we could see that the discharge coefficient for the orifice2 of nozzle-0 was the highest to compensate the mass flow. Thus the orifice will experience a higher flow rate than it would if the both orifices were functioning normally, which eventually results in a strong hole to hole fluctuation within a nozzle which can significantly affect the global spray characteristics and finally the combustion and emission process in engines.

4.2.2. Injection pressure effects on discharge coefficient

Fig. 8 presents the variations of the discharge coefficient at different injection pressures. The average value at each operating point was obtained by determining the mean of the instantaneous values during the intermediate stages of the injection process. As discussed earlier the discharge coefficient for orifice1 of nozzle-0 was observed to be significantly lower compared to all other orifices at all injection pressures. In particular, for nozzle-0 it could be seen that the discharge coefficient for orifice1 decreased marginally with injection pressure, while the C_d for orifice2 increases marginally with injection pressure. For the normal nozzle (nozzle-1) it could be seen in Fig. 8 the changes in C_d for the orifices with injection pressures were negligible, thus, the injection pressure has no significant effect on the variation of nozzle discharge coefficient. As discussed earlier it could also be seen that the C_d for orifice2 of nozzle-0 was considerably greater than that of all other orifices at all injection pressures.

4.3. Injection rate

Figs. 9 and 10 represent the injection rate obtained over the entire period of injection. The injection rate was derived from the transient values of the measured momentum flux and injection

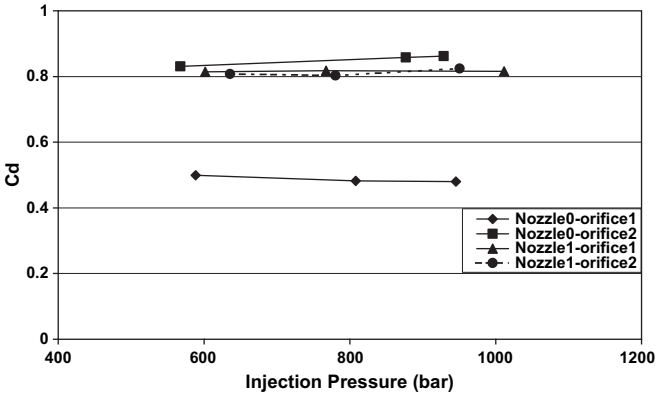

Fig. 8. Variation of time averaged nozzle discharge coefficient at different injection pressures.

pressure. Thus, most of the transients observed in the momentum flux and the injection pressure measurements were reflected, particularly during the early stages of the injection rate profiles. However, the transients occurring during the intermediate stages of the injection period were less pronounced in this case. As discussed earlier the injection rate profile of nozzle-1 is greater than that of nozzle-0. The problem of impeded flow for orifice1 of nozzle-0 has been reflected again with the derived injection rate as shown in Fig. 9 (a), whose magnitude is significantly lower than that of all other orifices.

4.3.1. Injection velocity

The injection velocity was obtained by averaging the time resolved injection velocity, obtained from equation (1), over the

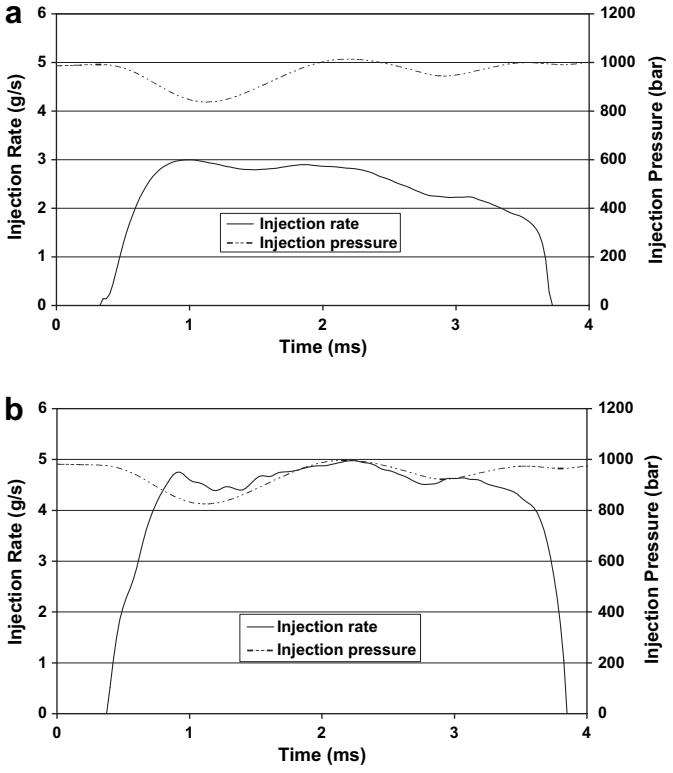

Fig. 9. (a) Variation of injection rate for orifice1 of nozzle-0 at an injection pressure of 1000 bar. (b) Variation of injection rate for orifice2 of nozzle-0 at an injection pressure of 1000 bar.

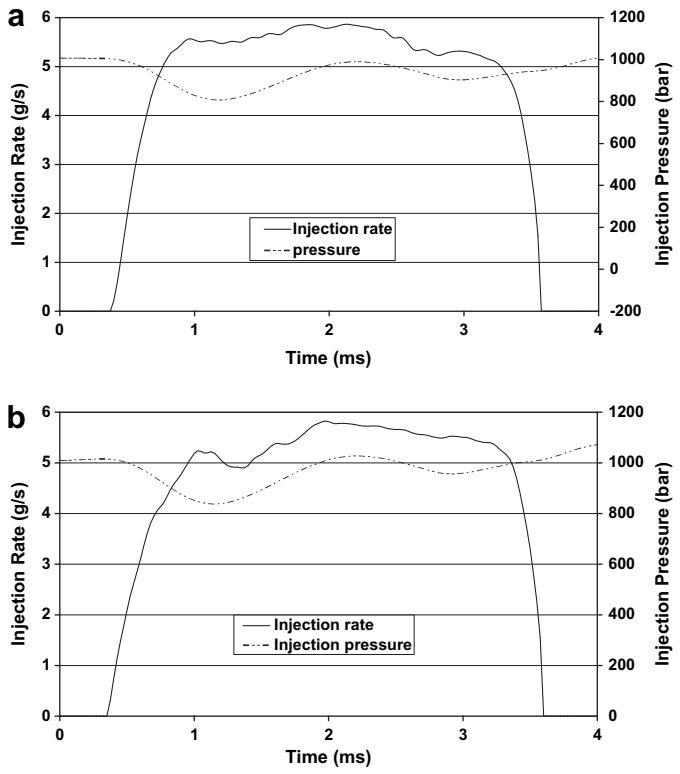

Fig. 10. (a) Variation of injection rate for orifice1 of nozzle-1 at an injection pressure of 1000 bar. (b) Variation of injection rate for orifice2 of nozzle-1 at an injection pressure of 1000 bar.

injection cycle. The influence of cavitation on the actual flow has not been considered in the calculations of the injection velocity. Under cavitating conditions the velocities could be higher due to the decrease in the effective area of the liquid spray with respect to conservation of mass. However, the intensity of cavitation for the nozzles used in this investigation may be less compared to sharp inlet nozzles due to hydro-grinding of their inlet geometry. Fig. 11 represents the velocity at different injection pressures. The velocity of the injected jet was observed to increase linearly with the increase in injection pressure for all the orifices. The velocity of the impeded flow of orifice1 of nozzle-0 was observed to be significantly lower than that of all other orifices. The injection velocity of the jet from orifice2 of nozzle-0 was only marginally greater (of the order of 20 m/s) than that of all other orifices under different

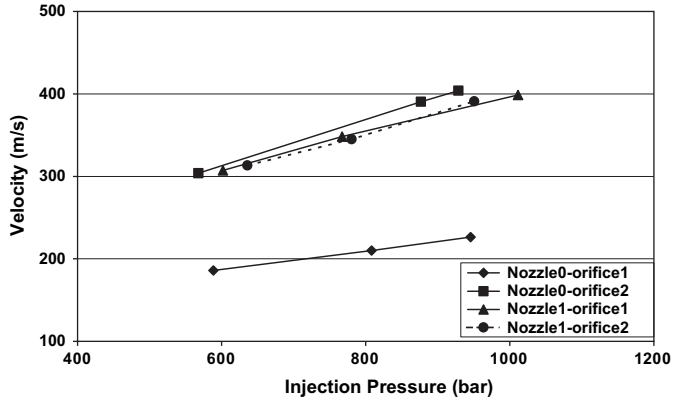

Fig. 11. Variation of time averaged velocity at different injection pressures.

injection pressures. The changes in the jet velocities with injection pressures were marginally greater for orifice2 of nozzle-0 than that of all other orifices. No considerable difference in the jet velocities was observed between the orifices of nozzle-1. Moreover, the differences in the velocities between the orifices of nozzle-1 and of orifice2 of nozzle-0 were not significant.

4.4. Influence of impingement distance

The influence of impingement distance on the characteristic parameters such as momentum flux, nozzle discharge coefficient,

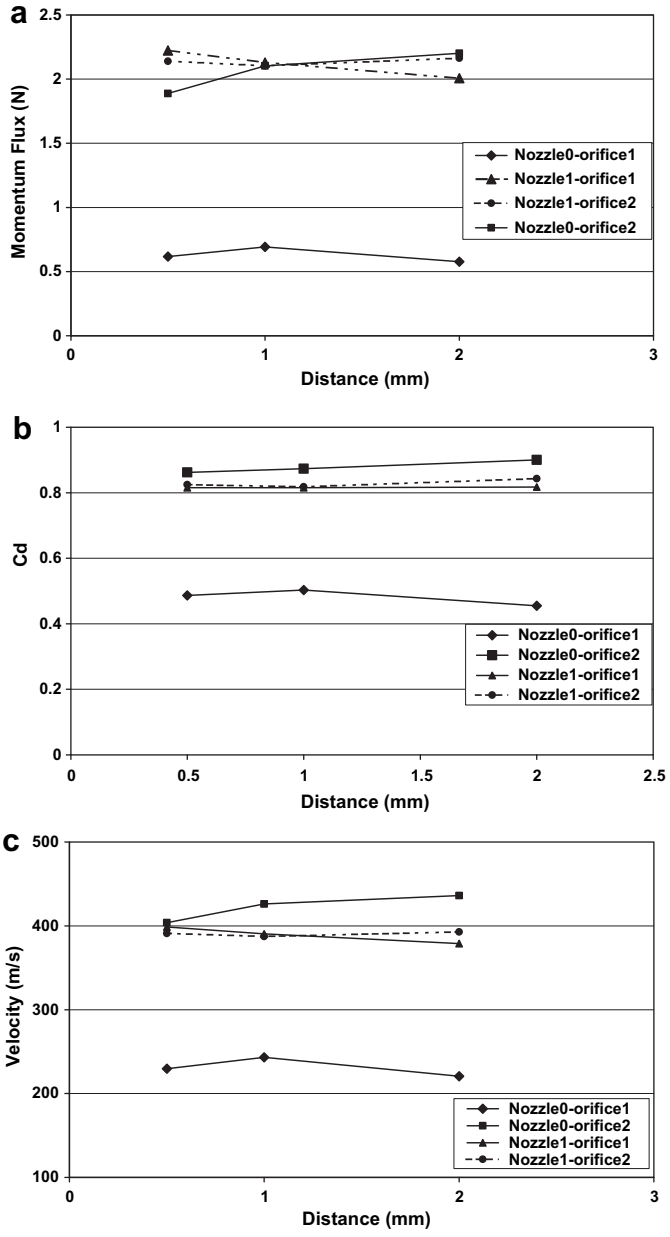

Fig. 12. (a) Variation of time averaged momentum flux measured at different impingement distances from the nozzle tip at an injection pressure of 1000 bar. (b) Variation of time averaged nozzle discharge coefficients derived from momentum flux measured at different impingement distances from the nozzle tip at an injection pressure of 1000 bar. (c) Variation of time averaged velocity of the jet derived from momentum flux measured at different impingement distances from the nozzle tip at an injection pressure of 1000 bar.

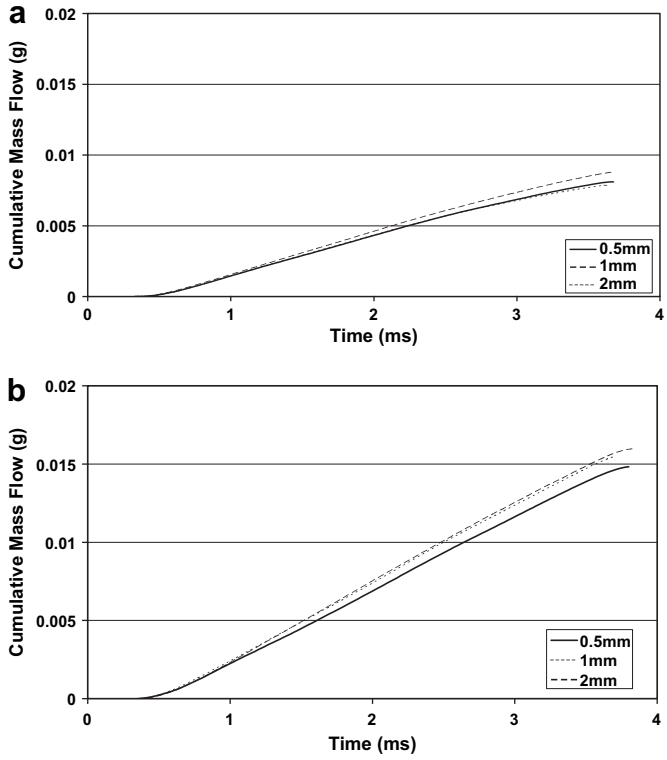

Fig. 13. (a) Cumulative mass flow for orifice1 of nozzle-0 obtained from momentum flux measured at different impingement distances from the nozzle tip at an injection pressure of 1000 bar, (b) Cumulative mass flow for orifice2 of nozzle-0 obtained from momentum flux measured at different impingement distances from the nozzle tip at an injection pressure of 1000 bar.

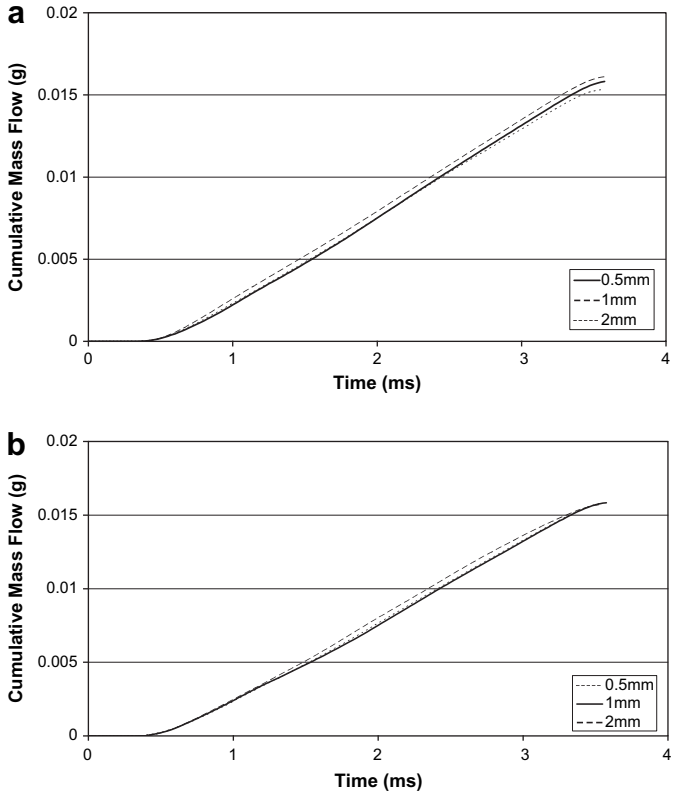

Fig. 14. (a) Cumulative mass flow for orifice1 of nozzle-1 obtained from momentum flux measured at different impingement distances from the nozzle tip at an injection pressure of 1000 bar, (b) Cumulative mass flow for orifice2 of nozzle-1 obtained from momentum flux measured at different impingement distances from the nozzle tip at an injection pressure of 1000 bar.

injection velocity and injected mass from the nozzle orifices are discussed in Figs. 12–14 respectively.

4.4.1. Momentum flux

Fig. 12 (a) shows the influence of impingement distances on the time averaged momentum flux measurements. No consistent trend of the momentum flux variation with the impingement distance could be seen. Nozzle-0 and Nozzle-1 exhibit a different trend, the momentum flux of the jet from the orifices of nozzle-0 was observed to increase from 0.5 mm to 1 mm distance. While the momentum flux of the jet issuing from the orifices of nozzle-1 exhibits a decreasing trend as the impingement distance increases from 0.5 mm to 1 mm. It could be seen that for an impingement distance of about 1 mm; the momentum fluxes of the orifices of nozzle-1 and the orifice2 of nozzle-0 are nearly overlapping one another. The variation of the momentum flux with the impingement distance for orifice1 of nozzle-0 was very marginal at different impingement distances, however the momentum flux of orifice2 of nozzle-0 was observed to increase slightly with much lesser gradient between 1 mm and 2 mm impingement distances. Similarly, the variations in the momentum flux of the jets from the orifices of nozzle-1 were marginal when compared at the impingement distance of 1 mm.

4.4.2. Discharge coefficient

Fig. 12 (b) shows the influence of impingement distance on the time averaged nozzle discharge coefficient. In general the variations in the discharge coefficient for all orifices with respect to the impingement distances were negligible. For nozzle-0 it could be seen that there were marginal variations in the C_d from 1 mm to 2 mm, besides these variations no considerable changes in C_d could be observed for orifices of nozzle-1 with different impingement distances. As discussed earlier, the C_d of orifice1 of nozzle-0 was lower compared to all other orifices and it is reflected for all three impingement distances.

4.4.3. Injection velocity

Fig. 12 (c) shows the variation of the time average injection velocity at different impingement distances. It could be seen that the jet velocities derived at an impingement distance of 0.5 mm for the orifices of nozzle-1 and for the orifice2 of nozzle-0 were almost similar. The variations in the time averaged velocity for nozzle-1 at different impingement distances were very negligible compared to nozzle-0.

4.4.4. Injection rate

Figs. 13 and 14 compares the cumulative mass flows for each orifice at the operating point of 1000 bar injection pressure for varying distances from the nozzle. In Fig. 14 (b) it could be seen that for orifice2 of nozzle-1 that the variation of the impingement distance from 0.5 to 2 mm has no significant effects on the derived injection rate and moreover the derived values were still within the normal injection to injection fluctuating limits and the derived cumulative mass was approximate 0.0158 g per injection cycle. Similarly in Fig. 13 (a) it could be seen that the total injected mass flow derived at 0.5 mm and 2 mm impingement distances were on top of each other and derived a total mass of about 0.008 g per injection cycle and the injection mass derived from the impingement distance of 1 mm was about 0.0088 g per injection cycle. It

could be seen that the variation in the cumulative mass flow was within 10%. Similarly, it could be seen in Fig. 13 (b) the derived cumulative mass flow at an impingement distance of 1 mm and 2 mm are more or less overlapping each other. The total mass flow at the two operating points were approximately 0.0154 g and 0.016 g per injection cycle and the total mass obtained from an impingement distance of 0.5 mm was lower than that of 1 mm and 2 mm impingement distance and it was about 0.0148 g per injection cycle. But still it could be seen that maximum variation in the derived cumulative mass flow was roughly about 10%. Similarly, in Fig. 14 (a) it could be seen that the cumulative mass flow derived for different distances from the nozzle are well within 5%. For the impingement distances of 0.5 mm and 1 mm distances, the curves are much closer to each other and the total mass flow was 0.016 g per cycle compared to 0.0153 g per cycle for an impingement distance of 2 mm. From the above discussions it could be seen that the impingement distances up to 2 mm has no significant effect on the measurements and the maximum variation that was observed in this measurement for these two nozzles were only within 4–12%.

5. Conclusions

The impingement technique was applied to two multi-orifice common rail diesel injector nozzles with different geometrical configurations. The technique was able to characterise the nozzle geometry and the near nozzle spray characteristics. The transients of the needle motion, dynamics of the pressure fluctuations were all reflected in the momentum flux measurements. This technique was able to identify malfunctioning orifices of nozzles which are bound to have an adverse effect on engine performance and emissions. This technique proves to be a vital tool for predicting the performance of nozzle flows with different geometrical configurations and to understand the variations that may arise in emissions from similar nozzles. Other findings are summarised as follows:

- The momentum of the spray was observed to be proportional to the fluctuations in injection pressure in a single injection cycle and so are the injection rates and the instantaneous velocities.
- The characteristics of the momentum flux obtained over an injection cycle are different for all the orifices and the rate of increase of momentum with pressure varies between the orifices of the same nozzle but the magnitudes of the averaged momentum flux, injection rate and the injection velocity vary indistinctly between the orifices of the same nozzle.
- The injection pressures as well as its fluctuations had no significant influence on the discharge coefficient of the nozzle orifices.
- The discharge coefficient was observed to be higher during the needle opening stages compared to the intermediate stage of an injection cycle.
- The transients of the spray were unique for an orifice.
- No distinct variation in averaged discharge coefficient could be observed between the nozzles with two different orifice outlet diameters but same inlet rounding.
- The impingement distances had no significant influence on the derived injected mass.

References

[1] N. Rajaratnam, Turbulent Jets, Elsevier Scientific Company, 1974.
[2] J.M. Desantes, R. Payri, J.M. Pastor, J. Gimeno, Experimental characterization of internal nozzle flow and diesel spray behavior. Part 1. Non-evaporative conditions, Fuel 84 (5) (2005) 553–556.
[3] L.C. Ganippa, S. Andersson, J. Chomiak, Transient Measurements of Discharge Coefficient of Diesel Nozzles, SAE Paper 2000-01-2788, 2000.
[4] T. Husberg, V. Manente, R. Ehleskog, S. Anderson, Fuel Flow Impingement Measurements on Multi-Orifice Diesel Nozzles, SAE Paper 2006-01-1552, 2006.
[5] J.M. Desantes, R. Payri, F.J. Salvador, J. Gimeno, Measurements of Spray Momentum for the Study of Cavitation in Diesel Injection Systems, SAE Paper 2003-01-0703, 2003.
[6] D. Siebers, B. Higgins, Flame Lift-off on Direct Injection Diesel Sprays under Quiescent Conditions, SAE Paper 2001-01-0530, 2001.
[7] S. Cheong, J. Lui, D. Shu, J. Wang, Effects of Ambient Pressures on Dynamics of Near-nozzle Diesel Spray Studied by Ultrafast X-radiography, SAE Paper 2004-01-2026, 2004.

Nomenclature

A_0:	Cross Sectional Area of the Flow
C_d:	Discharge Coefficient
F(t):	Instantaneous Impingement Force
m(t):	Instantaneous Mass Flow Rate
$\dot{m}(t)$:	Actual Mass Flow Rate
$\dot{m}_{theo}(t)$:	Theoretical mass Flow rate
ΔP(t):	Instantaneous Change in Pressure
ΔV(t):	Instantaneous Change in Velocity
ρ:	Fuel Density